

Carbon Dioxide Capture Using Ionic Liquids Containing Amino Acid-Type Anions. Effect of the Cation, Anion on the Absorption Efficiency

Gabriela Barbosa-Moreno¹, Nohra V. Gallardo-Rivas*¹, Rafael Martínez-Palou*²

¹Tecnológico Nacional de México/Instituto Tecnológico de Ciudad Madero. Prol. Bahía de Aldhair y Av. de las Bahías, 89600, Altamira, Tamaulipas, México.

²Instituto Mexicano del Petróleo. Gerencia de Investigación en Desarrollo de Catalizadores y Productos Químicos. Eje Central Lázaro Cárdenas 152. 07730 CDMX, México.

*Corresponding author: Nohra V. Gallardo-Rivas, email: nohvigari@itcm.edu.mx; Rafael Martínez-Palou, email: rpalou@imp.mx

Received June 30th, 2022; Accepted November 15th, 2022.

DOI: <http://dx.doi.org/10.29356/jmcs.v68i1.1827>

Abstract. In this work, the synthesis of twelve ionic liquids (ILs) with imidazolium cation and amino acid-derived anions and their evaluation as carbon dioxide (CO₂) absorbents both, in pure form and aqueous solution (30 % of water) are reported and compared with monoethanolamine (MEA), which is a well-known commercial absorbent with wide application in the Petroleum Industry for capturing acid gases. The effect of both cation substituent features such as length and unsaturation of alkyl chains and amino acid structure at the anion on the CO₂ absorption efficiency was studied. All the ILs displayed good CO₂ absorption efficiency, being the ILs derived from 1-octyl-3-vinylimidazolium the most effective for this purpose, especially with lysinate anion ([OVI][L]); a capture rate of 1501 mg CO₂/mol of IL was achieved when it was diluted in water (30 %).

Keywords: Carbon dioxide; ionic liquids; amino acids type anions; absorption.

Resumen. En este trabajo se reporta la síntesis de doce líquidos iónicos (LIs) con el catión imidazolio y los aniones derivados de aminoácidos y la evaluación de estos compuestos como absorbentes de dióxido de carbono (CO₂), tanto empleando los absorbentes puros, como en solución acuosa (30 % de agua). Los resultados se comparan con los obtenidos con monoetanolamina (MEA), que es un conocido absorbente comercial con amplia aplicación en la Industria del Petróleo en la captura de gases ácidos. Se estudió el efecto de las características de ambos *N*-sustituyentes de los cationes, como la longitud y la presencia de insaturación en las cadenas de alquilo y la estructura de aminoácidos que conforman los aniones de los LIs estudiados, en la eficiencia de absorción de CO₂. Todos los LIs mostraron una buena eficiencia de absorción de CO₂, siendo los LIs derivados del 1-octil-3-vinilimidazolio los más efectivos para este fin, especialmente con el anión lisinato ([OVI][L]); se logró una tasa de captura de 1501 mg CO₂/mol de LIs cuando el absorbente se diluyó en agua (30 %).

Palabras clave: Dióxido de carbono; líquidos iónicos; aniones derivados de aminoácidos; absorción.

Introduction

The main energy source for humanity has arisen from non-renewable fossil compounds, which when used, generate some acid gases, from which CO₂ is the most abundant and contributes greatly to the greenhouse

effect. The production of this gas is not only increased by the point mentioned above, but also by other factors such as the burning of coal in power plants or combustion of diesel in engines and devices based on this fuel type, which turn out to be very frequent and harmful emission sources [1,2].

The economic development of countries, especially those in the process of growth, is closely linked to an increase in energy demand; therefore, projections indicate that the need for fossil fuels will continue growing given the world population soaring trend, which is why the development of novel environmentally and economically efficient technologies is more and more necessary [3].

Among the main options to achieve the reduction of CO₂ emissions, the efficiency improvement of conventional generating plants, better control over energy consumption, use of greater proportions of renewable resources, and capture and storage of CO₂ are found, where the last alternative is the most feasible and possible to develop today, and for this reason, it has been playing an important role in the last century [4-6].

Different processes such as pre-, post-, and oxy-combustion have been developed to capture CO₂ [7,8]. One of the advantages of post-combustion capture is that since it occurs after combustion and before CO₂ is released into the atmosphere, it can be implemented in facilities that are still in operation [9]. In this context, absorption is considered within this capture stage; in this process, chemical solvents trigger an acid-based chemical reaction, where alkanolamines are among the best-known compounds. Primary amines are very reactive with CO₂, but they are also more corrosive and sensitive to degradation, so secondary and tertiary amines are used to reduce these characteristics [10,11].

Ionic liquids (ILs), which are known as “green solvents” due to their low toxicity, practically zero vapor pressure and high solvent capacity, have been noted as promising candidates to remove CO₂ through absorption because of their high thermal stability, negligible steam pressure and adjustable physicochemical properties [12-18]. ILs exhibit strong affinity to CO₂, which stems from the possibility of varying cations or anions by adding functional groups, especially those containing amino groups [19-23]. It has been proven that when functionalized ILs are dissolved, they can greatly reduce viscosity [24]. The absorption capacity of most ILs solutions with a functional group with basic properties has been widely reported with absorption values higher than 0.5 mol of CO₂/mol of IL, including anions derived from amino acids [24-29]. The study of the absorption capacity of some amino acids was previously compiled [1,19,30]. Since 2010, Gurkan et al. showed that methioninate and proline trihexyl(tetradecyl)phosphonium absorb CO₂ in nearly 1:1 stoichiometry [31]. Recently, two reviews have shown the potential of ILs for CO₂ capture and utilization, mechanisms, and nature of interactions between ILs and CO₂ in terms of cation and anion nature, economic analysis, and perspectives of using ILs for this application [32,33].

In this work, the synthesis of ILs with imidazolium cation and amino acid anions is described and the efficiency of these compounds as absorbers performing CO₂ capture is evaluated with the aim of making a comparative study of the effect of the cation and substituents of the amino acid structure (anion) to obtain a prototype with high capture efficiency. In addition, the effect of diluting ILs with water on the absorption efficiency and concomitant cost reduction of the CO₂ capture process is studied by comparing it with the one stemming from using methyl ethyl amine, which is widely used in the Oil Industry as absorbent of acid gases. It was observed that IL [OVI][L] could be regenerated by a simple methodology and reused in several absorption cycles without noticeable absorption capacity loss.

Experimental

Reagents and materials

All reagents (Aldrich) were used without further purification. FT-IR spectra were obtained on a Perkin Elmer Spectrum 100 spectrophotometer with 4 cm⁻¹ spectral resolution and 16 scans using an attenuated total reflection accessory with diamond plate.

The ¹H NMR (400 MHz) and ¹³C NMR (100 MHz) spectra were recorded on an Ascend 400 NMR equipment from Bruker Avance III Console using tetramethylsilane (TMS) as internal standard and deuterated water (D₂O) as solvent at room temperature. EI mass spectra were recorded on GC-Mass Spectrometer Agilent 5973N. For the CO₂ desorption studies, a CEM Discover monomode microwave synthesizer was used [34].

Synthesis of ILs with amino acid anions

The ILs containing an imidazolium-type cation and amino acid anions such as [OMI][AA], [BMI][AA] and [OVI][AA] were synthesized by alkylation reactions of the imidazole derivatives, exchange of the halogenated anion by hydroxyl and subsequent neutralization using the amino acids (AA) Lysine [L], Arginine [A], Glutamine [G], and Histidine [H], which were obtained according to the standard procedure described below.

1-vinyl-3-octylimidazolium bromide [OVI][Br] was prepared by the reaction between 1-vinylimidazole (0.1 mol) and *n*-octylbromide (0.15 mol) in a round-bottom flask with magnetic stirring at 50°C for 4 h without solvent. The resulting IL was washed twice with ethyl acetate (1:4 v/v) and vacuum dried at 50°C for 5 h. The anion exchange of Br by OH was carried out through the equimolar reaction between [OVI][Br] and KOH dissolved in EtOH under stirring at 5°C for 4 h and subsequently filtered to remove the KBr obtained as by-product.

Then, 0.10 mol of [OVI][OH] and the corresponding AA (0.12 mol) were mixed in deionized water (50 mL) at room temperature for 4 h with magnetic stirring. Afterward, water was distilled under vacuum and the product was diluted in ethanol (20 mL) to remove the excess of AA, filtered and ethanol was removed from the solution under vacuum, yielding [OVI][L]. Following the procedure described above with the corresponding reagents, the compounds shown in Table 1 were obtained.

Table 1. ILs synthesized in this study.

Entry	Cation	Anion	Identification
1	1-Butyl-3-methylimidazolium	Lysinate	[BMI][L]
2		Arginate	[BMI][A]
3		Glutamate	[BMI][G]
4		Histidinate	[BMI][H]
5	1-Methyl-3-Octylimidazolium	Lysinate	[OMI][L]
6		Arginate	[OMI][A]
7		Glutamate	[OMI][G]
8		Histidinate	[OMI][H]
9	1-Octyl-3-Vinylimidazolium	Lysinate	[OVI][L]
10		Arginate	[OVI][A]
11		Glutamate	[OVI][G]
12		Histidinate	[OVI][H]

The structure and high purity of the synthesized compounds was confirmed FT-IR spectrometry, ¹H and ¹³C NMR as described below.

[BMI][L]. Following the experimental procedure a viscous light-yellow liquid was obtained (yield: 82 %). FT-IR (neat) ν (cm⁻¹): 3295, 2965, 2931, 2865, 1634, 1592, 1434, 1390, 1368, 1345, 1090, 1050, 879, 782, 729, 663. EI Mass spectrum: C₁₄H₂₉N₄O₂: 284 (Calcd., 284). ¹H NMR (400 MHz, D₂O) δ 8.67 (s, 1H), 7.42 (s, 1H), 7.37 (s, 1H), 4.13 (t, *J* = 7.0 Hz, 2H), 3.83 (s, 3H), 3.21 (t, *J* = 6.9 Hz, 1H), 2.81 (t, *J* = 6.9 Hz, 2H), 1.78 (q, *J* = 7.2 Hz, 2H), 1.54 (m, 6H), 1.28 (m, 2H), 0.84 (t, *J* = 7.0 Hz, 3H) ppm. ¹³C NMR (101 MHz, D₂O) δ 182.41, 135.98, 123.48, 122.23, 55.72, 49.32, 39.74, 35.79, 33.81, 31.33, 28.36, 22.13, 18.83, 12.79 ppm.

[BMI][A]. Following the experimental procedure a viscous light-yellow liquid was obtained (yield: 91 %). FT-IR (neat) ν (cm^{-1}): 3306, 2967, 2929, 2867, 1664, 1601, 1448, 1403, 1379, 1345, 1091, 1052, 878, 783, 730, 663. EI Mass spectrum: $\text{C}_{14}\text{H}_{28}\text{N}_6\text{O}_2$: 312 (Calcd., 312). ^1H NMR (400 MHz, D_2O) δ 8.71 (s, 1H), 7.46 (s, 1H), 7.40 (s, 1H), 4.15 (t, $J = 7.1$ Hz, 2H), 3.85 (s, 3H), 3.18 (m, 1H), 1.79 (q, $J = 7.1$ Hz, 2H), 1.55 (m, 4H), 136 (m, 2H), 0.85 (t, $J = 7.1$ Hz, 3H) ppm. ^{13}C NMR (101 MHz, D_2O) δ 182.95, 157.31, 135.99, 123.53, 122.28, 55.67, 49.36, 41.20, 35.89, 31.37, 24.76, 18.88, 12.86 ppm.

[BMI][G]. Following the experimental procedure a viscous light-yellow liquid was obtained (yield: 88 %). FT-IR (neat) ν (cm^{-1}): 3270, 2967, 2957, 2873, 1640, 1587, 1454, 1433, 1380, 1374, 1091, 1052, 879, 784, 760, 661. EI Mass spectrum: $\text{C}_{13}\text{H}_{24}\text{N}_4\text{O}_3$: 284 (Calcd., 284). ^1H NMR (400 MHz, D_2O) δ 8.69 (s, 1H), 7.44 (s, 2H), 7.39 (s, 2H), 4.15 (t, $J = 7.1$ Hz, 2H), 3.85 (s, 3H), 3.53 (t, $J = 5.9$ Hz, 1H), 2.32 (t, $J = 7.8$ Hz, 2H), 1.96 (q, $J = 6.9$ Hz, 2H), 1.79 (q, $J = 7.1$ Hz, 2H), 1.36–1.13 (m, 2H), 0.86 (t, $J = 7.3$ Hz, 3H) ppm. ^{13}C NMR (101 MHz, D_2O) δ 178.06, 174.29, 135.88, 123.51, 122.26, 54.72, 49.34, 35.83, 31.35, 29.83, 25.45, 18.86, 12.81 ppm.

[BMI][H]. Following the experimental procedure a viscous light-yellow liquid was obtained (yield: 88 %). FT-IR (neat) ν (cm^{-1}): 3284, 2966, 2930, 2865, 1642, 1591, 1444, 1407, 1374, 1371, 1091, 1051, 878, 802, 756, 677, 660. EI Mass spectrum: $\text{C}_{14}\text{H}_{24}\text{N}_5\text{O}_2$: 293 (Calcd., 292). ^1H NMR (400 MHz, D_2O) δ 8.71 (s, 1H), 7.61 (s, 1H), 7.46 (s, 1H), 7.41 (s, 1H), 6.88 (s, 1H), 4.16 (t, $J = 7.1$ Hz, 2H), 3.86 (s, 3H), 3.45–3.55 (m, 1H), 2.90–2.96 (m, 1H), 2.75–2.81 (m, 1H), 1.80 (q, $J = 7.2$ Hz, 2H), 1.24–1.31 (m, 2H), 0.86 (t, $J = 7.1$ Hz, 3H) ppm. ^{13}C NMR (101 MHz, D_2O) δ 174.12, 136.42, 135.79, 132.29, 123.53, 122.29, 116.72, 54.81, 49.36, 35.90, 35.90, 31.38, 28.23, 18.89, 12.87 ppm.

[OMI][L]. Following the experimental procedure a viscous light-yellow liquid was obtained (yield: 78%). FT-IR (neat) ν (cm^{-1}): 3285, 3162, 3064, 2964, 2862, 1656, 1583, 1471, 1372, 1328, 1180, 1101, 1043, 984, 884, 732, 715, 643, 629, 474. EI Mass spectrum: $\text{C}_{18}\text{H}_{37}\text{N}_4\text{O}_2$: 340 (Calcd., 340). ^1H NMR (400 MHz, D_2O) δ 8.82 (s, 1H), 7.47 (s, 1H), 7.45 (s, 1H), 4.17 (t, $J = 7.0$ Hz, 2H), 3.86 (s, 3H), 3.20 (t, $J = 5.6$ Hz, 1H), 2.76 (t, $J = 7.0$ Hz, 2H), 1.78–1.82 (m, 2H), 1.46–1.54 (m, 4H), 1.26–1.34 (m, 2H), 1.15–1.23 (m, 10H), 0.73 (t, $J = 6.1$ Hz, 3H). ^{13}C NMR (101 MHz, D_2O) δ 182.84, 135.96, 123.68, 122.23, 55.80, 49.58, 39.85, 35.93, 34.13, 31.46, 29.63, 28.98, 28.73, 28.60, 25.78, 22.34, 22.19, 13.74.

[OMI][A]. Following the experimental procedure a viscous light-yellow liquid was obtained (yield: 85 %). FT-IR (neat) ν (cm^{-1}): 3280, 3169, 3118, 2961, 2851, 1670, 1574, 1469, 1391, 1286, 1189, 1074, 1044, 1000, 870, 773, 710, 670, 628, 485. EI Mass spectrum: $\text{C}_{18}\text{H}_{36}\text{N}_6\text{O}_2$: 368 (Calcd., 368). ^1H NMR (400 MHz, D_2O) δ 8.68 (s, 1H), 7.41 (s, 1H), 7.37 (s, 1H), 4.11 (t, $J = 7.1$ Hz, 2H), 3.82 (s, 3H), 3.13 (m, 3H), 1.78 (m, 2H), 1.53 (m, 4H), 1.18 (m, 10H), 0.74 (t, $J = 7.1$ Hz, 3H) ppm. ^{13}C NMR (101 MHz, D_2O) δ 183.12, 156.97, 135.60, 123.52, 122.19, 55.51, 49.57, 41.05, 35.73, 31.72, 31.13, 29.31, 29.23, 28.36, 28.19, 25.44, 24.56, 22.10, 13.52 ppm.

[OMI][G]. Following the experimental procedure a viscous light-yellow liquid was obtained (yield: 83 %). FT-IR (neat) ν (cm^{-1}): 3330, 3176, 3107, 2966, 2861, 1658, 1568, 1471, 1383, 1327, 1190, 1099, 1049, 985, 880, 730, 691, 632, 471. EI Mass spectrum: $\text{C}_{17}\text{H}_{32}\text{N}_4\text{O}_3$: 340 (Calcd., 340). ^1H NMR (400 MHz, D_2O) δ 8.64 (s, 1H), 7.3 (s, 3H), 7.35 (s, 3H), 4.10 (t, $J = 7.1$ Hz, 2H), 3.81 (s, 3H), 3.60 (t, $J = 7.0$ Hz, 1H), 2.34 (t, $J = 6.9$ Hz, 2H), 1.98 (q, $J = 6.9$ Hz, 2H), 1.75–1.81 (m, 2H), 1.15–1.21 (m, 10H), 0.75 (t, $J = 7.0$ Hz, 3H) ppm. ^{13}C NMR (101 MHz, D_2O) δ 177.82, 175.29, 135.84, 123.48, 122.18, 54.39, 49.57, 35.67, 31.03, 29.73, 29.21, 28.25, 28.06, 26.99, 25.34, 22.03, 13.46 ppm.

[OMI][H]. Following the experimental procedure a viscous light-yellow liquid was obtained (yield: 81 %). FT-IR (neat) ν (cm^{-1}): 3272, 3138, 3088, 2960, 2860, 1667, 1563, 1443, 1406, 1339, 1169, 1083, 1061, 1000, 880, 750, 706, 655, 620, 482. EI Mass spectrum: $\text{C}_{18}\text{H}_{32}\text{N}_5\text{O}_2$: 349 (Calcd., 348). ^1H NMR (400 MHz, D_2O) δ 8.66 (s, 1H), 7.59 (s, 1H), 7.38 (s, 1H), 7.35 (s, 1H), 6.89 (s, 1H), 4.08 (t, $J = 7.0$ Hz, 2H), 3.79 (s, 3H), 3.72 (m, 1H), 3.03 (m, 1H), 2.90 (m, 1H), 1.74 (m, 2H), 1.14 (m, 10H), 0.71 (t, $J = 7.0$ Hz, 3H) ppm. ^{13}C NMR (101 MHz, D_2O) δ 176.22, 136.21, 135.80, 132.61, 123.52, 122.17, 117.18, 55.24, 49.55, 35.73, 31.15, 29.37, 29.32, 28.38, 28.21, 25.46, 22.11, 13.54 ppm.

[OVI][L]. Following the experimental procedure a viscous light-yellow liquid was obtained (yield: 71 %). FT-IR (neat) ν (cm⁻¹): 3277, 2943, 2926, 2859, 1657, 1595, 1457, 1377, 1349, 1138, 1105, 1092, 1050, 881, 730, 660. EI Mass spectrum: C₁₉H₃₇N₄O₂: 349 (Calcd., 349). ¹H NMR (400 MHz, D₂O) δ 9.13 (s, 1H), 7.79 (s, 1H), 7.58 (s, 1H), 7.12 (dd, J = 3.4, 15.3 Hz, 1H), 5.77 (d, J = 7.1 Hz, 1H), 5.37 (d, J = 6.6 Hz, 1H), 4.21 (t, J = 7.1 Hz, 2H), 3.21 (t, J = 6.0 Hz, 1H), 2.82 (t, J = 7.2 Hz, 2H), 1.82 (m, 2H), 1.52 (m, 4H), 1.37 (m, 2H), 1.18 (m, 10H), 0.73 (t, J = 6.9 Hz, 3H) ppm. ¹³C NMR (101 MHz, D₂O) δ 181.73, 134.35, 128.24, 122.99, 119.59, 109.45, 55.43, 50.02, 39.39, 33.44, 31.26, 29.32, 28.51, 28.36, 27.39, 25.57, 22.19, 21.87, 13.61 ppm.

[OVI][A]. Following the experimental procedure a viscous light-yellow liquid was obtained (yield: 79 %). FT-IR (neat) ν (cm⁻¹): 3287, 2958, 2922, 2858, 1658, 1589, 1459, 1374, 1350, 1164, 1113, 1088, 1049, 882, 764, 663 ppm. EI Mass spectrum: C₁₉H₃₆N₆O₂: 380 (Calcd., 380). ¹H NMR (400 MHz, D₂O) δ 9.17 (s, 1H), 7.82 (s, 1H), 7.58 (s, 1H), 7.17 (dd, J = 3.2, 15.3 Hz, 1H), 5.79 (d, J = 7.2 Hz, 1H), 5.40 (d, J = 6.7 Hz, 1H), 4.22 (t, J = 7.2 Hz, 2H), 3.14 (m, 1H), 3.08 (m, 2H), 1.83 (m, 2H), 1.51 (m, 4H), 1.15-1.25 (m, 10H), 0.74 (t, J = 6.9 Hz, 3H) ppm. ¹³C NMR (101 MHz, D₂O) δ 183.02, 156.73, 134.65, 128.58, 123.37, 119.92, 109.63, 55.64, 50.06, 41.01, 31.65, 31.56, 29.30, 28.53, 28.47, 25.63, 24.50, 22.19, 13.69 ppm.

[OVI][G]. Following the experimental procedure a viscous light-yellow liquid was obtained (yield: 75 %). FT-IR (neat) ν (cm⁻¹): 3301, 2945, 2926, 2860, 1660, 1576, 1452, 1381, 1295, 1175, 1100, 1096, 1054, 876, 725, 672. EI Mass spectrum: C₁₈H₃₂N₄O₃: 352 (Calcd., 352). ¹H NMR (400 MHz, D₂O) δ 9.15 (s, 1H), 7.80 (s, 1H), 7.58 (s, 1H), 7.15 (dd, J = 3.2, 15.1 Hz, 1H), 5.78 (d, J = 7.2 Hz, 1H), 5.39 (d, J = 7.2 Hz, 1H), 4.21 (t, J = 7.0 Hz, 2H), 3.68 (t, J = 6.7 Hz, 1H), 2.36 (t, J = 6.9 Hz, 2H), 2.04 (q, J = 6.9 Hz, 2H), 1.80-1.86 (m, 2H), 1.15-1.24 (m, 10H), 0.73 (t, J = 6.8 Hz, 3H). ¹³C NMR (101 MHz, D₂O) δ 178.62, 174.08, 134.56, 128.41, 123.27, 119.60, 109.54, 54.49, 50.04, 31.37, 30.86, 29.41, 28.51, 28.47, 26.25, 25.60, 22.19, 13.65 ppm.

[OVI][H]. Following the experimental procedure a viscous light-yellow liquid was obtained (yield: 73 %). FT-IR (neat) ν (cm⁻¹): 3301, 2945, 2926, 2860, 1660, 1576, 1452, 1381, 1295, 1175, 1100, 1096, 1054, 876, 725, 672. EI Mass spectrum: C₁₉H₃₂N₅O₂: 361 (Calcd., 361). ¹H NMR (400 MHz, D₂O) δ 9.19 (s, 1H), 7.84 (s, 1H), 7.65 (s, 1H), 7.58 (s, 1H), 7.18 (dd, J = 3.3, 15.2 Hz, 1H), 6.9 (s, 1H), 5.81 (d, J = 7.1 Hz, 1H), 5.42 (d, J = 6.9 Hz, 1H), 4.23 (t, J = 7.1 Hz, 2H), 3.85 (t, J = 6.9 Hz, 1H), 3.07-3.14 (m, 1H), 2.95-3.01 (m, 1H), 1.80-1.90 (m, 2H), 1.20-1.26 (m, 10H), 0.74 (t, J = 7.1 Hz, 3H). ¹³C NMR (101 MHz, D₂O) δ 174.08, 136.43, 134.73, 132.42, 128.65, 123.42, 120.05, 116.73, 109.78, 55.10, 50.10, 31.33, 29.29, 28.51, 28.37, 28.29, 25.66, 22.20, 13.85 ppm.

ILs regeneration and reutilization

The CO₂ could be removed from the saturated ILs (5.0 g) by heating in a microwave oven monomodal (CEM Discover) at 70 °C at 85 W of power for 5 minutes in closed-vessel mode. The CO₂ desorption was verified by ¹H NMR and FT-IR.

Procedure for the quantification of CO₂ absorption using the ILs-AA

The absorption tests were carried out at 303 K using an initial pressure of 3 atm. The apparatus consists of a stainless-steel gas tank equipped with a digital manometer and subjected to constant stirring; the diagram is shown in Fig. 1. The temperature is controlled by a thermostat placed in the heating bath (\pm 0.1 K variation). The variation in gas pressure was approximately \pm 0.001 atm throughout the pressure interval ranging from 1 to 3 atm. 10.0 g of pure ILs or 30 % dissolved in water were introduced into the tank and hermetically sealed. Air was then removed from the system by means of a vacuum pump that was connected to the system for 15 min (ultimate vacuum was $1.3 \cdot 10^{-5}$ atm). Subsequently, CO₂ was loaded into the tank and the absorption process began with stirring (150 rpm). The system was considered in steady state once the pressure remained constant for half an hour. The concentration of absorbed CO₂ was determined using the ideal gas equation of state. Each experiment was performed in triplicate, which had an approximate uncertainty of 0.02 mol CO₂/mol IL. The absorption curves were obtained by measuring the system pressure drop every 2 min. The experiments with ILs and MEA were carried out under the same experimental conditions.

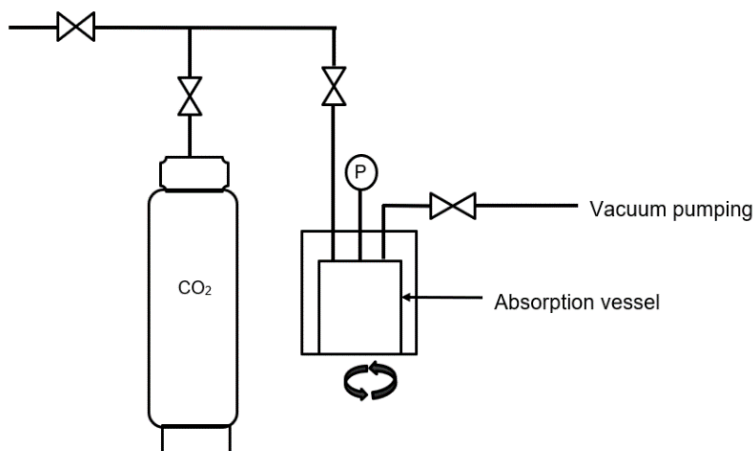


Fig. 1. Schematic representation of the equipment used to determine CO₂ absorption.

Results and discussion

Synthesis of AA functionalized ILs

Table 1 The synthesis general scheme of the ILs functionalized with AA is described in Fig. 2.

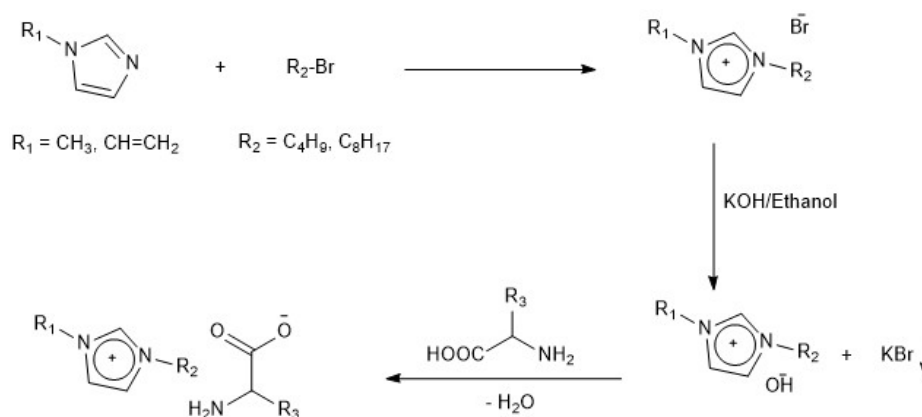


Fig. 2. Synthesis scheme of the ILs functionalized with AA.

The synthesis of the precursor IL [RMI][X] (R = *n*-C₄H₉, *n*-C₈H₁₇ and vinyl; MI = *N*-methylimidazolium; X = Cl, Br) began with the alkylation of 1-methylimidazole (0.1 mol) with the corresponding alkyl halide (0.15 mol) in an inert atmosphere for 48 h with heating and magnetic stirring. The anion exchange reaction to replace the halide by hydroxyl was carried out using potassium hydroxide (KOH) in ethanol at low temperatures to form the precursor IL [RMI][OH], which was subsequently neutralized with AA to obtain the ILs shown in Table 1. The employed amino AAs were selected because they present more than one basic site in their structure, which as expected favors the capture of an acid gas as CO₂ [15,19,22,24].

The results of the IR analysis are shown in Figures 3, 4 and 5.

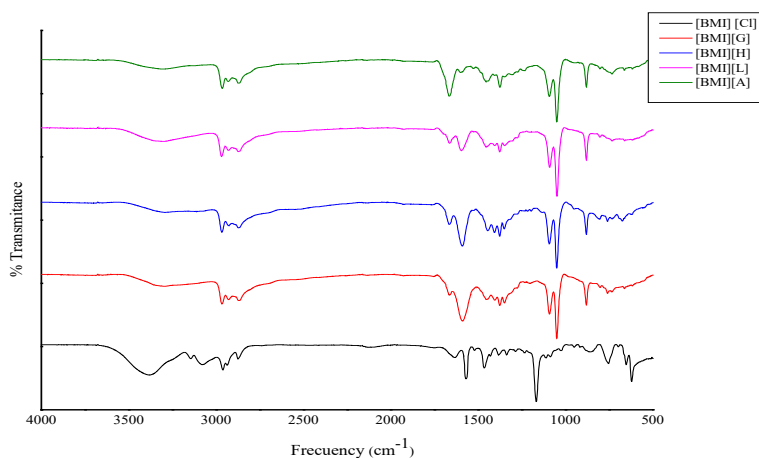


Fig. 3. FTIR spectra of pure ionic liquids corresponding to [BMI][AA] and [BMI][Cl].

Fig. 3 shows a broad peak in the [BMI][Cl] spectrum centered at 3378 cm^{-1} reveals the presence of water in the halogenated IL. Halogens are strong proton acceptors, and this band is the result of the overlapping absorption bands due to symmetric (ν_1) and asymmetric (ν_3) stretching vibrational modes of water molecules, which is strongly red-shifted, reflecting the strong hydrogen bond interaction ($\text{Cl}^- \dots \text{H-O-H} \dots \text{Cl}^-$). The signal centered on 2872 cm^{-1} is due to vibrations of C-H of methylene and methyl groups in the alkyl chains. The bands in the range between $3000\text{--}3200\text{ cm}^{-1}$ are mainly assigned to $+\text{C}(2)\text{-H}$ stretching mode and the intense band at 1166 cm^{-1} correspond to the skeletal vibrational mode of the imidazolium ring [35,36]. The band observed in the AA-containing ILs at $3500\text{--}3100\text{ cm}^{-1}$ is attributed to the -NH groups and is overlapped by the -OH stretching in the AA structure. Also, at 1590 cm^{-1} , a CO_2^- pronounced stretching band was observed in the AA-functionalized ILs. An imidazole C-N stretching peak appeared at $1000\text{--}1100\text{ cm}^{-1}$. Finally, the bands between $3000\text{--}2800\text{ cm}^{-1}$, $1450\text{--}1460\text{ cm}^{-1}$ and around 1350 cm^{-1} correspond to the vibrational modes of C-H the alkyl chains of the cation (symmetric and asymmetric stretching and bending) [37,38].

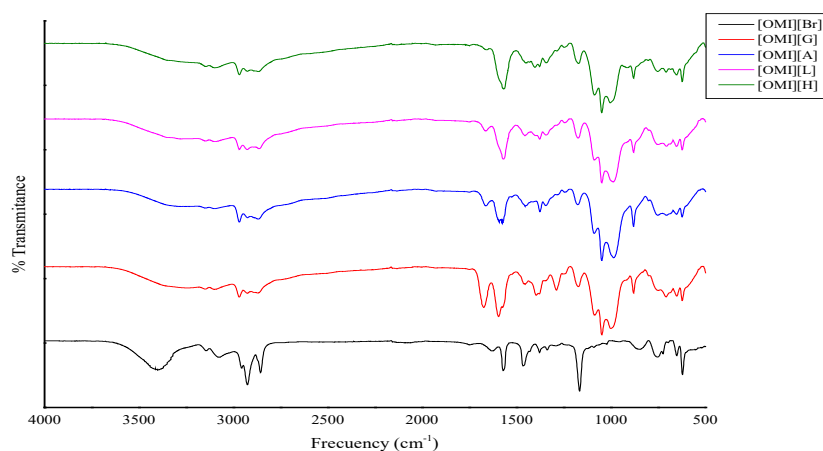


Fig. 4. FTIR spectrum of pure ionic liquids corresponding to [OMI][AA] and [OMI][Br].

Because the only structural difference between of ILs [BMI][AA] (Fig. 3) and [OMI][AA] series (Fig. 4) is the length of the alkyl chain bonded to the Nitrogen-1 of the imidazolium ring, only slight differences between the spectra shown in figures 3 and 4 can be seen in the regions related to the bands in the region 3000-2800 cm^{-1} , 1430-1460 cm^{-1} and 1320-1380 cm^{-1} which correspond to the vibrational C-H modes of the alkyl chains (symmetric and asymmetric stretching and bending) as observed by other authors [37,38]. At 1570 cm^{-1} , a CO_2^- pronounced stretching band was observed in the functionalized AA-functionalized ILs.

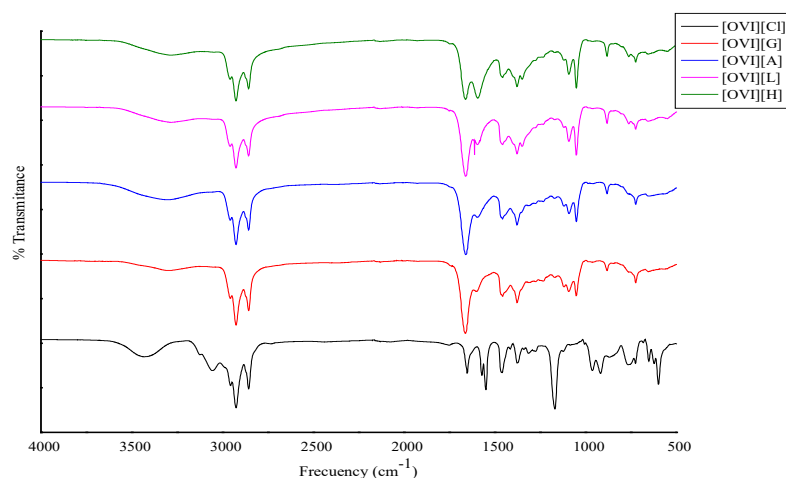


Fig. 5. FTIR spectrum of pure ionic liquids corresponding to [OVI][AA].

Similarly, to Fig. 3 and 4, Fig. 5 shows a broad peak in the [OVI][Cl] spectrum, centered at 3395 cm^{-1} , which corresponds to the overlapping absorption bands due to symmetric (ν_1) and asymmetric (ν_3) stretching vibrational modes of water molecules. A wide band is observed in the AA-functionalized ILs at 3500-3100 cm^{-1} , which is attributed to the -NH groups, and is overlapped with the -OH stretching in the AA structure. The bands located at 3200-3000 cm^{-1} and 1166 cm^{-1} correspond to the vibrational modes of the imidazolium ring (symmetric and asymmetric stretching). At 3045 cm^{-1} , a medium stretching band is observed, which corresponds to the =CH₂ of the vinyl group. The signal situated at 1688 cm^{-1} is attributed to the C=C stretching band of the vinyl group. Also, at 1570 cm^{-1} , a CO_2^- pronounced stretching was observed in the AA-functionalized ILs. Finally, the bands between 3000-2800 cm^{-1} , 1450-1460 cm^{-1} and 1350 cm^{-1} correspond to the vibrational modes of the alkyl chains of the cation (symmetric and asymmetric stretching and bending). As expected, the most noticeable differences between the series of spectra in Fig. 5 with Figures 3 and 4 lie fundamentally in the signals related to =CH₂ of the vinyl group and the C=C bands described previously.

Absorption of CO₂ by the synthesized ILs. Effect of the cation structure

Following the procedure described in the experimental section, the absorption capacity of pure ILs was evaluated at 25 °C and 40 °C. At a temperature of 40 °C, the absorptions follow the same trend than at 25 °C, but the amount of CO₂ absorbed is slightly higher, fundamentally due to the reduction in the viscosity of the ILs, which favors a better interaction between the absorbent and the gas (higher diffusivity). Entries 1-8 shows the absorption results of the functionalized ILs in nitrogen-3 with butyl ([BMI]) and octyl ([OMI]) group with the same four AAs in both cases. It is observed that the absorption values tend to be higher for the AA-functionalized IL with octyl substituent. This result is due to the viscosity of the ILs containing the 1-methyl-3-octylimidazolium cation is lower than the ILs with 3-butyl substituent; this favors the improved interaction efficiency between CO₂ and the IL [3,7].

Feng et al. studied the absorption in AA-functionalized ILs mixture with methyldiethanolamine (MDEA). They found that adding amino acid IL greatly reinforced the CO₂ absorption of MDEA in aqueous solution over a wide range of IL concentration (5-100 %), partial pressure (0.04-4.0 atm) and temperature between 20-40 °C.

Aqueous solution with 15 % IL + 15 % MDEA had higher absorption rate and larger uptake capacity. The higher temperature led to the larger reaction rate and less viscosity [39].

In another study of CO₂ absorption with AA-containing ILs, it was shown that the absorption capacity of the evaluated ILs decreases with increasing temperature between 20 and 80 °C, demonstrating that it is possible to desorb the CO₂ gas under CO₂-rich conditions by temperature-swing absorption [40].

Hiremath et al. have observed a decrease in CO₂ adsorption capacity of silica-supported ILs when the temperature in the experiments was increased from 20 to 100 °C [41].

Table 2. Results of CO₂ absorption by the ILs studied without dilution at 25 °C and 40 °C.

Entry	Identification	Absorption capacity of the ILs without dilution (mmol CO ₂ / mol IL)	
		25 °C	40 °C
1	[BMI][L]	821.47	873.64
2	[BMI][A]	788.58	839.27
3	[BMI][G]	761.94	811.73
4	[BMI][H]	748.32	800.52
5	[OMI][L]	719.25	772.36
6	[OMI][A]	708.47	759.43
7	[OMI][G]	902.62	950.59
8	[OMI][H]	891.55	943.67
9	[OVI][L]	1121.37	1173.85
10	[OVI][A]	1072.84	1124.44
11	[OVI][G]	1042.29	1093.57
12	[OVI][H]	1031.09	1079.63

On the other hand, when comparing the different octyl substituted, it is observed that the vinyl group played a relevant role in the effectiveness of these ILs, which exceeded 1000 mmol CO₂/mol IL in all cases [12]. The effect of the vinyl substituent can probably be explained through the formation of a π - π system between the unsaturated groups of the IL and CO₂, which makes the sorbent-CO₂ interaction more effective. In all cases, a possible electrostatic interaction between the electron rich oxygen atoms in CO₂ and electron deficient heterocycle, that could favor a supramolecular structure between ILs and CO₂, can take place (Fig. 6) [29].

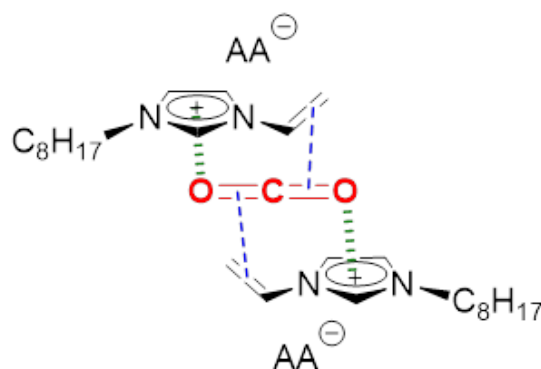


Fig. 6. Possible π - π and electrostatic interaction between [OVI][AA] and CO₂.

Effect of the anion structure on the absorption capacity of the ILs

As shown in Table 2, although the results did not follow the same trend with all the cations, it is evident that the lysinate anion presented the highest adsorption capacity, which seems to be related to the presence of two primary amino groups that result in two strong basic sites capable of interacting more effectively with CO₂, showing that the chemisorption is the more dominant mechanism in our AA-containing ILs.

Fig. 7 shows the ¹³C NMR spectrum of [BMI][L] before and after CO₂ adsorption, where two additional signals appear at 166.74 and 163.75 ppm, respectively, which correspond to the formation of carbamic acids from both amino groups, thus confirming the existence of chemisorption between CO₂ and the IL anion.

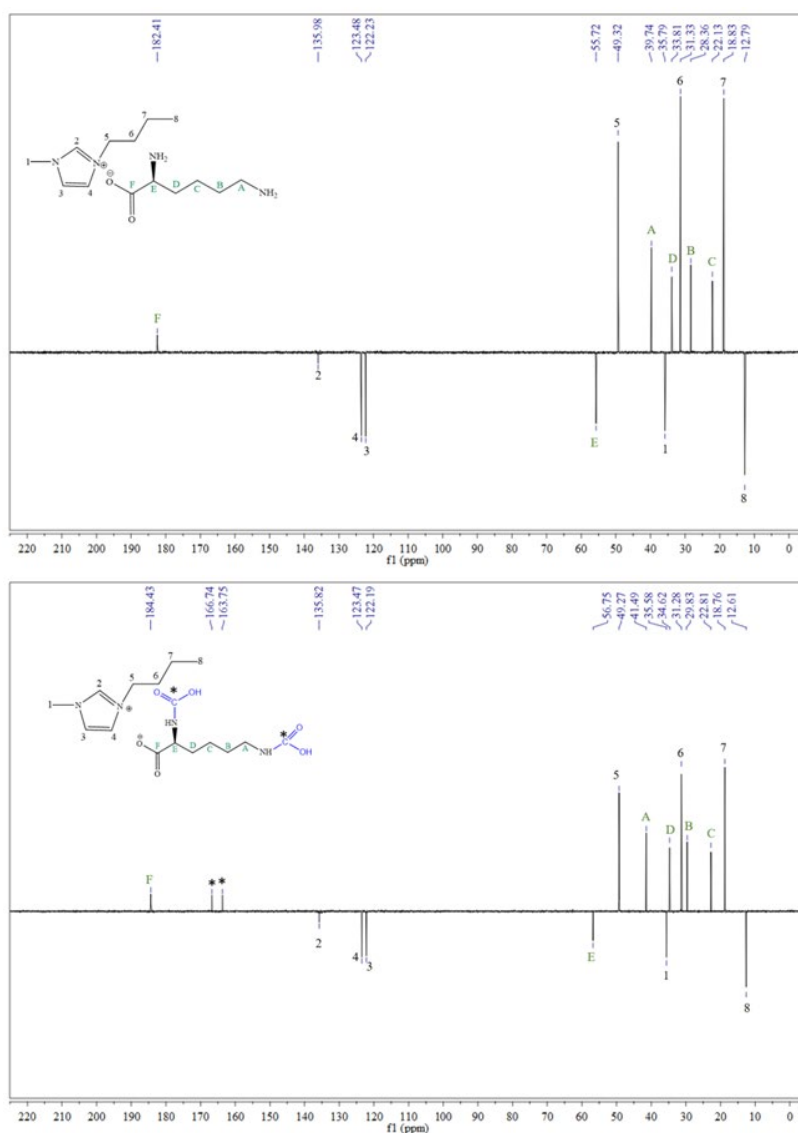


Fig. 7. ¹³C NMR spectrum of [BMI][L] before and after CO₂ absorption.

The chemisorption was also confirmed by the presence of a new FTIR band that appeared after CO₂-IL interaction around 1785 cm⁻¹ and is attributed to the asymmetric C=O vibration of the former carbamate species, as have been observed by us (Fig. 8) and other authors [37,38]. Also, the noticeable decrease in the broad band at 3000–3600 cm⁻¹, assigned to νN–H and νO–H vibrations, and the bands at 1580 and 1400 cm⁻¹ attributed to ν(COO⁻)_{sym.} and ν(COO⁻)_{assym.}, respectively, confirm the carbamate formation [42].

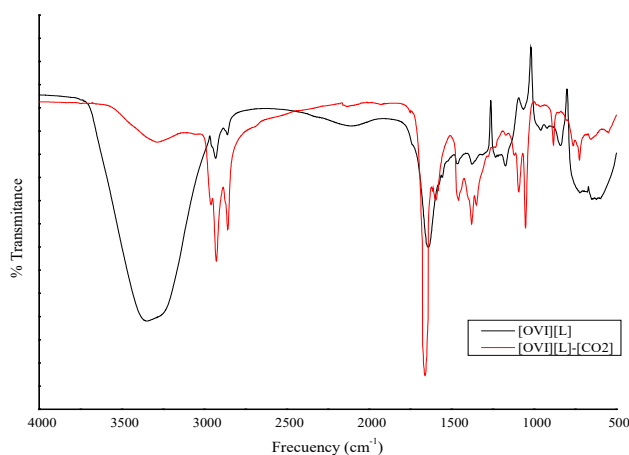


Fig. 8. FT-IR spectrum of [BMI][L] before and after CO₂ absorption.

Effect of dilution on the adsorption capacity of the ILs

Fig. 9 shows a comparison between the absorption capacity of monoethanolamine (MEA) and functionalized ILs-AA diluted at 30 % in water. As can be seen, the solubility of CO₂ is clearly favored after dilution in water even though the solvent absorption under these conditions is practically nil, but in the case of solutions, in addition to chemisorption, the physisorption process is also favored [20,26,30,37].

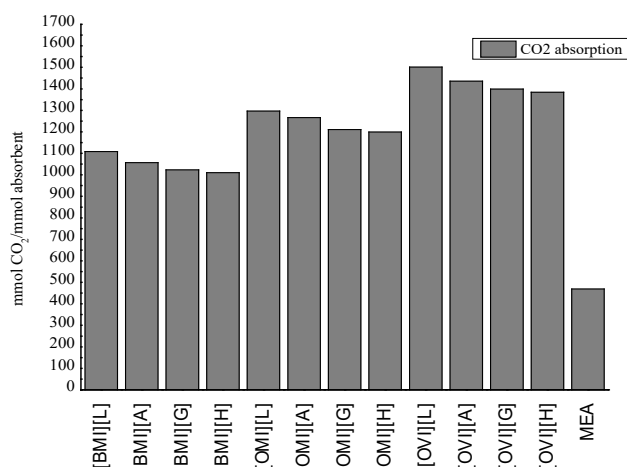


Fig. 9. Absorption capacity of the ILs-AA in 30 % mass of aqueous solution.

Fig.10 shows the CO₂ absorption curves of [OVI][AA] diluted at 30 % wt. in water, which were the most effective ILs.

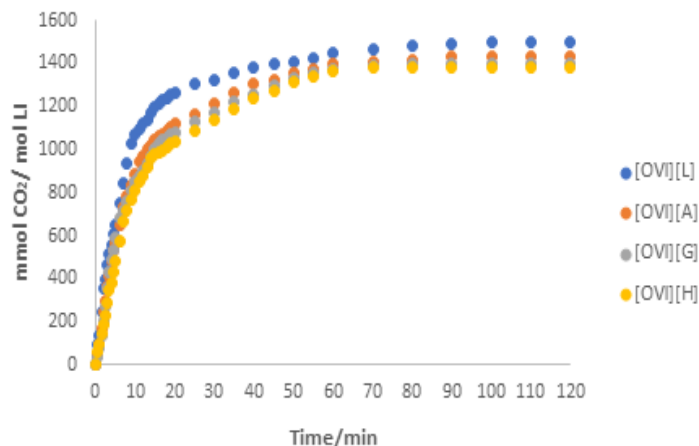


Fig. 10. CO₂ uptake with [OVI] and the different amino acids in 30 % wt. solution.

According to the results shown in Table 2 and Fig. 9, the CO₂ capture efficiency for ILs with the same cation ([BMI], [OMI] or [OVI]), and AAs-containing anions follows the order: [Cation][L] > [Cation][A] > [Cation][G] > [Cation][H]. This order is inversely proportional to the $pK_{a(NH_2)}$ of the corresponding AAs, confirming that the basicity of the amino groups plays a key role the CO₂ capture (Table 3).

Table 3. pK_{NH_2} of the AAs used in this study [42].

AA	$pK_{a(NH_2)}$
Lysine	8.95
Arginine	9.04
Glutamine	9.13
Hystidine	9.17

Fig. 11 shows the CO₂ absorption curves of the different cations with lysinate anion diluted at 30 % wt. in water to appreciate the difference in their activity. The 30 % concentration was selected because it is the concentration commonly applied in the amine-assisted CO₂ capture in Mexican Oil Industry. This concentration achieves an adequate cost/performance ratio of the chemical treatment. On the other hand, it is known that low viscosity obtained after IL dissolution and a weaker cation-anion interaction in the IL solution are the dominant factors responsible of the higher CO₂ capture.

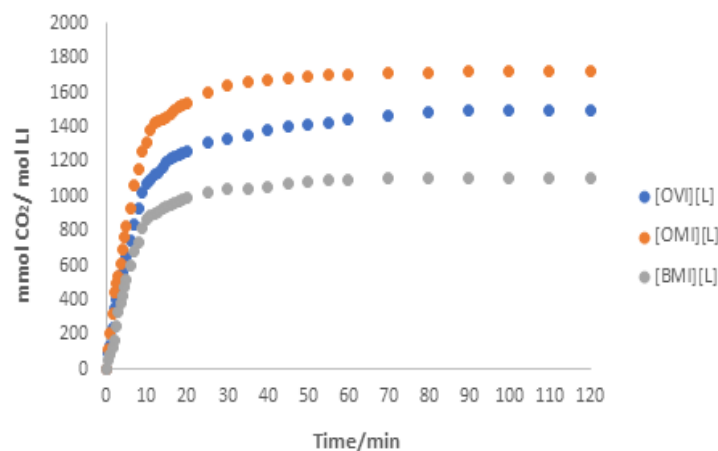


Fig. 11. CO₂ uptake with [L] and the different cations of ILs in 30 % wt. solution.

Fig. 12 shows the CO₂ pressure drop because of the absorption of the lysinate ILs with the different cations, in comparison with MEA at the same dilution. It can be observed that the kinetics of the absorption process is very similar in the case of the ILs, but the highest absorption was obtained in the case of cation with unsaturated substituent ([OVI]).

Considering that the time until a constant pressure was reached is directly linked with the absorption kinetics, the quicker a constant pressure level is reached, the faster is the absorption. Consequently, the absorption kinetics of lysinate-containing ILs was faster than MEA, which is probably due to the presence in the lysinate anion with two amino groups in each molecule of the ILs compared to one amine group in the MEA, coupled with the probable electrostatic π - π interactions that can be favored between the ILs and CO₂ [26].

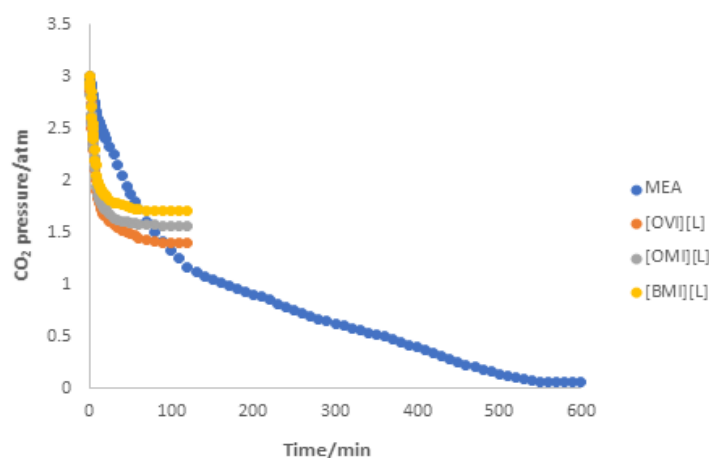


Fig. 12. Absorption kinetics of lysine derivatives compared to MEA (30 % wt. solution).

In the case of dilution experiments, the lysinate ILs showed the highest performance for CO₂ capture, particularly [OVI][L]. The better performance of the lysinate ILs is probably due to the position of the two amino groups in the anion that favor greater basicity and adequate nucleophilicity and a more effective

interaction of these groups with CO₂. Fig. 13 shows the possible interactions that favor the better performance of [OVI][L], even when there is no convincing evidence to confirm this proposal. [29].

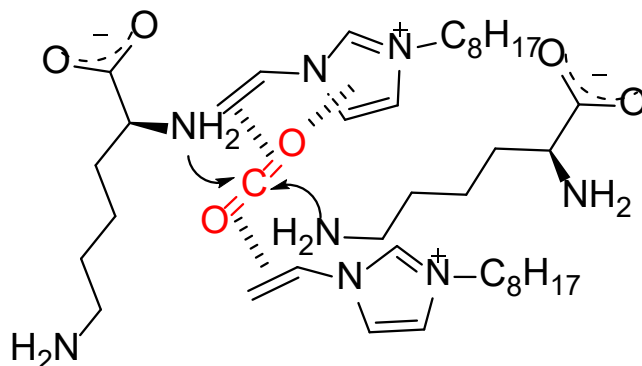


Fig. 13. Probable interactions between CO₂ and [OVI][L].

Chemisorption between CO₂ and carboxylate groups in 1,3-dialkylimidazolium has also been demonstrated, which explains the high performance shown by AA containing ILs [42].

Interestingly, [OVI][L] is a monomer that can be polymerized to obtain the corresponding poly(IL). It has been shown that poly(ILs) are also excellent CO₂ absorbers [43,44]. The study of the absorption properties of poly([OVI][L]) is currently underway in our research group.

According to our observations and those of other authors, the main interactions that favor CO₂ absorption are acid-base interactions (CO₂⋯NH₂, chemisorption), and the electrostatic interactions that can occur between ILs and CO₂. The electrostatic interaction could explain why many non-amino functionalized ILs can absorb a significant amount of CO₂ (physisorption) [1,29,33].

Regeneration and reuse of [OVI][L] after the first adsorption cycle

Following the procedure described in the Experimental Part, it was demonstrated that CO₂ can be desorbed from [OVI][L] and the IL can be reused in five consecutive absorption/desorption cycles without considerable loss of its adsorption capacity (Table 4).

Table 4. Results of CO₂ absorption of [OVI][L] under five cycles of absorption/desorption.

Cycle	Absorption capacity (mmol CO ₂ / mol IL)
1	1121
2	1119
3	1120
4	1114
5	1111
6	1103

Conclusions

Twelve ILs with three imidazole-based cations and four amino acid-derived anions were synthesized and evaluated as CO₂ sorbents. The ILs with the 1-octyl-3-vinylimidazolium cation gave the best adsorption results and the lysinate anion was found to give the ILs the highest adsorption capacity, attributable to the adequate disposition of the primary amino groups that favor a better interaction with CO₂. The performance of the anions correlated inversely with their pK_{a(NH₂)}. The CO₂ solubility was favored with dilution of the ILs in water, which was attributed to the decrease in the medium viscosity, thus favoring the sorbent-CO₂ interaction, and to the combination of chemisorption and physisorption processes. The ¹³C NMR and FT-IR spectrum of [BMI][L] confirmed the chemisorption through the detection of signals corresponding to carbamic acids. [OVI][L] proved to be the best adsorbent, especially after dilution (30 % in water). The better performance of [OVI][L] is probably due to the more adequate distribution of the two amino groups in the aliphatic chain of the amino acid, which favors greater basicity and a more effective acid-base interaction of these groups with CO₂, coupled with the probably π - π and electrostatic interaction between CO₂ and the vinyl group. By comparing the obtained results with those concerning MEA, the ILs-AA displayed faster absorption kinetics. [OVI][L] can be regenerated under microwave irradiation and reutilized in several absorption cycles without appreciable loss of its absorption capacity, so this IL can be considered a viable alternative for application as solvent in post-combustion CO₂ capture from flue gas in fixed emission sources on a large scale.

Acknowledgements

G. Barbosa-Moreno wants to thank to CONACyT-México (511874/287475) for the degree fellowship granted. Furthermore, we appreciate the funding provided by the Tecnológico Nacional de México. The authors want to thank the Instituto Mexicano del Petróleo for the facilities granted in carrying out the experimental part of this work.

References

1. Torralba-Calleja, E.; Skinner, J.; Gutiérrez-Tauste, D. *J. Chem.* **2013**, 1–16. DOI: <http://dx.doi.org/10.1155/2013/473584>.
2. Zambrano-Monserrate, M. A. *Sci. Total Environ.* **2024**, 907, 167853. DOI: <https://doi.org/10.1016/j.scitotenv.2023.167852>.
3. Lecomte, F.; Broutin, P.; Lebas, A. CO₂ Capture Technologies to Reduce Greenhouse Gas Emissions, Ed. Technip, IFP Publications, 2010.
4. Rahman, F. A.; Aziz, M. M.; Saidur, R.; Bakar, W. A. Bakar, Hainin, M.; Putrajaya R.; Hassan, N. A. *Renew. Sustain. Energy Rev.* **2017**, 71, 112-116. DOI: <http://dx.doi.org/10.1016/j.rser.2017.01.011>.
5. Gray, M. L.; Hoffman, J. S.; Hreha, D. C.; Fauth, D. J.; Hedges, S. W.; Hedges, Champagne, K. J.; Pennline, H. W. *Energy Fuels* **2009**, 23, 4840-4844. DOI: <http://dx.doi.org/10.1021/ef9001204>.
6. Koytsoumpa, E. I.; Bergins, C.; Kakaras, E. *J. Supercrit. Fluids.* **2018**, 132, 3-16. DOI: <http://dx.doi.org/10.1016/j.supflu.2017.07.029>.
7. Kenarsari, S. D.; Yang, D.; Jiang, G.; Zhang, S.; Wang, J.; Rusell, A. G.; Wei, Q.; Fan, M. *RSC Adv.* **2013**, 45, 22739. DOI: <http://dx.doi.org/10.1039/C3RA43965H>.
8. Stanger, R.; Wall, T.; Spörl, R.; Paneru, M.; Grathwohl, S.; Weidmann, M.; Schefflmecht, G.; McDonald, D.; Myohanen, K.; Ritvanen, J.; Rahiala, S.; Hyppanen, T.; Mletzco, J.; Kather, A.; Santos, S. *Int. J. Greenhouse Gas Control.* **2015**, 40, 55–125. DOI: <http://dx.doi.org/10.1016/j.ijggc.2015.06.010>.
9. Romano, M. C. *Int. J. Greenhouse Gas Control.* **2013**, 18, 57-67. DOI: <http://dx.doi.org/10.1016/j.ijggc.2013.07.002>.

10. Blauwhoff, P. M.; Versteeg, G. F.; Van Swaaij, W. P. *Chem. Eng. Sci.* **1984**, *39*, 207-225. DOI: [http://dx.doi.org/10.1016/0009-2509\(84\)80021-4](http://dx.doi.org/10.1016/0009-2509(84)80021-4).
11. Vaidya, P. D.; Konduru, P.; Vaidyanathan, M.; Kenig, E. Y. *Ind. Eng. Chem. Res.* **2010**, *49*, 11067-11072. DOI: <http://dx.doi.org/10.1021/ie100224f>.
12. Saravanamurugan, S.; Kunov-Kruse, A. J.; Fehrmann, R.; Riisager, A. *Chem. Sus. Chem.* **2014**, *7*, 897-902. DOI: <http://dx.doi.org/10.1002/cssc.201300691>.
13. Ramdin, M.; De Loos, T. W.; Vlugt, T. J. *Ind. Eng. Chem. Res.* **2012**, *51*, 8149-8177. DOI: <http://dx.doi.org/10.1021/ie3003705>.
14. Luque, R.; Martínez-Palou, R. *Environm. Energy Sci.* **2014**, *7*, 2414-2447. DOI: <http://dx.doi.org/10.1039/c3ee43837f>.
15. Wan, M. M.; Zhu, H. Y.; Li, Y. Y.; Ma, J.; Liu, S.; Zhu, J. H. *ACS Appl. Mat. Interfaces.* **2014**, *6*, 12947-12955. DOI: <http://dx.doi.org/10.1021/am5028814>.
16. Zhang, X.; Zhang, X.; Dong, H.; Zhao, Z.; Zhang, S.; Huang, Y. *Energy Environ. Sci.* **2012**, *5*, 6668-6681. DOI: <http://dx.doi.org/10.1039/C2EE21152A>.
17. Martínez-Palou, R. *J. Mex. Chem. Soc.* **2007**, *51*, 252-264.
18. Bates, E. D.; Mayton, R. D.; Ntai, I.; Davis, J. H. *J. Am. Chem. Soc.* **2002**, *124*, 926-927. DOI: <http://dx.doi.org/10.1021/ja017593>.
19. Guzmán, J.; Ortega-Guevara, C.; De León, R. G.; Martínez-Palou, R. *Chem. Eng. Technol.* **2017**, *40*, 2339-2345. DOI: <http://dx.doi.org/10.1002/ceat.201600593>.
20. Shannon, M. S.; Bara, J. E. *Sep. Sci. Technol.* **2012**, *47*, 178-188. DOI: <http://dx.doi.org/10.1080/01496395.2011.630055>.
21. Carlisle, T. K.; Bara, J. E.; Gabriel, C. J.; Noble, R. D.; Gin, D. L. *Ind. Eng. Chem. Res.* **2008**, *47*, 7005-7012. DOI: <http://dx.doi.org/10.1021/ie8001217>.
22. Chen, X.; Luo, X.; Li, J.; Qiu, R.; Lin, J. *RSC Adv.* **2020**, *10*, 7751-7757. DOI: <http://dx.doi.org/10.1039/c9ra09293e>.
23. Wang, C.; Luo, X.; Zhu, X.; Cui, G.; Jiang, D.; Deng, D.; Li, H.; Dai, S. *RSC Adv.* **2013**, *3*, 15518-15527. DOI: <http://dx.doi.org/10.1039/C3RA42366B>.
24. Zhang, Y.; Wu, Z.; Chen, S.; Yu, P.; Luo, Y. *Ind. Eng. Chem. Res.* **2013**, *52*, 6069-6075. DOI: <http://dx.doi.org/10.1021/ie302928v>.
25. Ren, W.; Sensenich, B.; Scurto, A.M. *J. Chem. Thermodyn.* **2010**, *42*, 305-311. DOI: <http://dx.doi.org/10.1016/j.jct.2009.08.018>.
26. Feng, Z.; Yuan, G.; Xian-Kun, W.; Jing-Wen, M.; You-Ting, W.; Zhi-Bing, Z. *Chem. Eng. J.* **2013**, *223*, 371-378. DOI: <http://dx.doi.org/10.1016/j.cej.2013.03.005>.
27. Jing, G.; Zhou, L.; Zhou, Z. *Chem. Eng. J.* **2012**, *181-182*, 85-95. DOI: <http://dx.doi.org/10.1016/j.cej.2011.11.007>.
28. Sistla, Y. S.; Khanna, A. *Chem. Eng. J.* **2015**, *273*, 268-276. DOI: <http://dx.doi.org/10.1016/j.cej.2014.09.043>.
29. Zeng, S.; Zhang, X.; Bai, L.; Zhang, X.; Wang, H.; Wang, J.; Bao, D.; Li, M.; Liu, X.; Zhang, S. *Chem. Rev.* **2017**, *117*, 9625-9673. DOI: <https://doi.org/10.1021/acs.chemrev.7b00072>.
30. Martínez-Palou, R.; Likhanova, N. V.; Olivares-Xometl, O. *Pet. Chem.* **2014**, *54*, 595-607. DOI: <http://dx.doi.org/10.1134/S0965544114080106>.
31. Gurkan, B. E., de la Fuente, J. C., Mindrup, E. M., Ficke, L. E., Goodrich, B. F., Price, E. A., Schneider, W. F.; Brennecke, J. F. *J. Am. Chem. Soc.* **2010**, *132*, 2116-2117. DOI: <http://dx.doi.org/10.1021/ja909305t>.
32. Shukla, S. K., Khokarale, S. G., Bui, T. Q., Mikkola, J.-P. T. *Front. Mater.* **2019**, DOI: <http://dx.doi.org/10.3389/fmats.2019.00042>.
33. Aghaie, M.; Rezaei, N.; Zendeheboudi, S. *Renew. Sustain. Energy Rev.* **2018**, *96*, 502-525. DOI: <http://dx.doi.org/10.1016/j.rser.2018.07.004>.
34. CEM corp. web page: <https://www.cem.com>, accessed in September 2022.
35. Yamada, T.; Tominari, Y.; Tanaka, S.; Mizuno, M. *J. Phys. Chem. B* **2017** *121*, 3121-3129. DOI: <http://dx.doi.org/10.1021/acs.jpcc.7b01429>.

36. Yamada, T.; Tominari, Y.; Tanaka, S.; Mizuno, M.; Fukunaga, K. *Materials*. **2014**, 7, 7409–7422. DOI: <http://dx.doi.org/10.3390/ma7117409>.
37. Saravanamurugan, S.; Kunov-Kruse, A. J.; Fehrmann, R.; Riisager, A. *ChemSusChem*. **2014**, 7, 897–902. DOI: <http://dx.doi.org/10.1002/cssc.201300691>.
38. Ossowicz, P.; Kleboko, J.; Roman, B.; Janus, E.; Rozwadowski, Z. *Molecules*. **2019**, 24, 3252. DOI: <http://dx.doi.org/10.3390/molecules24183252>.
39. Feng, Z.; Cheng-Gang, F.; You-Ting, W.; Yuan-Tao, W.; Ai-Min, L.; Zhi-Bing, Z. *Chem. Eng. J.* **2010**, 160, 691–697. DOI: <http://dx.doi.org/10.1016/j.cej.2010.04.013>.
40. Cammarata, L.; Kazarian, S. G.; Salter, P. A.; Welton, T. *Phys. Chem. Chem. Phys.* **2001**, 3, 5192–5200. DOI: <http://dx.doi.org/10.1039/B106900D>.
41. Hiremath, V.; Jadhav, A. H.; Lee, H.; Kwon, S.; Seo, J. G. *Chem. Eng. J.* **2016**, 287, 602–617. DOI: <http://dx.doi.org/10.1016/j.cej.2015.11.075>.
42. <https://libroelectronico.uaa.mx/capitulo-4-aminoacidos-y/curvas-de-titulacion-de-los.html>, accessed in September 2022.
43. Gurau, G.; Rodriguez, H.; Kelley, S.P.; Janiczek, P.; Kalb, R.S.; Rogers, R.D. *Angew. Chem. Int. Ed.* **2011**, 50, 12024–12026. DOI: <http://dx.doi.org/10.1002/anie.201105198>.
44. Zulficar, S.; Sarwar, M. I.; Mecerreyes, D. *Polymer Chem.* **2015**, 6, 6435–6451. DOI: <http://dx.doi.org/10.1039/C5PY00842E>.
45. Shahrom, M. S. R.; Wilfred, C. D.; Taha, A.K.Z. *J. Mol. Liq.* **2016**, 219, 306–312. DOI: <http://dx.doi.org/10.1016/j.molliq.2016.02.046>.